Pinus nelsonii and a Cladistic Analysis of Pinaceae Ovulate Cone Characters

David S. Gernandt,[1] Calixto León-Gómez, Sergio Hernández-León, and Mark E. Olson

Departamento de Botánica, Instituto de Biología, Universidad Nacional Autónoma de México, A.P. 70-233, México,
Distrito Federal 04510 México.
[1]Author for correspondence (dgernandt@ibiologia.unam.mx)

Communicating Editor: Daniel Potter

Abstract—The complexity of ovulate cones and their preservation as fossils makes them promising material for reconstructing the evolutionary history of gymnosperms, but phylogenetic analyses of cone morphological characters of Pinaceae have been inconclusive. We describe the ovulate cone anatomy of *Pinus nelsonii*, a rare and phylogenetically isolated pinyon pine endemic to Mexico, and add the species together with *Pinus ponderosa* and the fossil *Pinus belgica* to a recoded and expanded ovulate cone morphology matrix for fossil and extant Pinaceae. The cone anatomy of *Pinus nelsonii* conforms to previous generic concepts of *Pinus*. Despite its phylogenetically isolated position among the soft pines (*Pinus* subgenus *Strobus*) and thus potential for displaying plesiomorphic features, the cone of *Pinus nelsonii* is unlike the oldest *Pinus* fossil cones in possessing enlarged, functionally wingless seeds partially embedded in scale tissue, and in lacking sclerenchyma in the cortex of the axis, in the bract, and in the scale. Cladistic analysis of cone morphology characters recovers several *Pityostrobus* species in a clade with *Pinus*. Although the inferred relationships among living species do not coincide in several respects to molecular studies, adding taxa and further exploration of characters promise to clarify relationships.

Keywords—Fossils, *Obirastrobus*, phylogeny, *Pityostrobus*, *Pseudoaraucaria*.

Anatomically preserved fossil ovulate cones from the Cretaceous and Cenozoic have been extremely influential in understanding past Pinaceae diversity (Miller 1976a; Smith and Stockey 2001, 2002). Most pinaceous fossil cones from the Cretaceous are classified in the extinct organ genera *Obirastrobus* Ohsawa, Nishida & Nishida (two described species), *Pityostrobus* Nathorst emend. Dutt (a polyphyletic assemblage of at least 28 anatomically described species), and *Pseudoaraucaria* Fliche (six species; Smith and Stockey 2002). Phylogenetic analyses of ovulate cone morphology characters suggest that these fossils are in the Pinaceae crown, but either few characters have been included (Alvin 1988; Shang et al. 2001) or strict consensus trees have been poorly resolved (Smith and Stockey 2001, 2002). Several strategies could be used to increase phylogenetic resolution. First, character coding decisions have an important influence on the results of phylogenetic analysis (Pleijel 1995; Hawkins 2000), and these decisions require further evaluation. Second, more fossil and extant taxa are available for inclusion in morphological analyses. Regarding extant pinaceous taxa, most have been treated as generic-level terminals, and consequently many characters have been scored as polymorphic (Alvin 1988; Smith and Stockey 2001, 2002; Gernandt et al. 2008). Dividing taxa with polymorphic character states into smaller units with monomorphic states (in this case, using species instead of genera) can reduce error in phylogenetic reconstructions (Nixon and Davis 1991). Third, adding characters can improve phylogenetic accuracy even when this requires including more missing data for some taxa (Wiens 2003). Fourth, through reciprocal illumination (Hennig 1966), hypotheses of homology based on morphological similarity can be assessed after phylogenetic analysis via congruence with other characters on a tree (Patterson 1982), and homoplasious characters can be identified for further study.

Pinus L. is by far the largest and most phylogenetically diverse genus in Pinaceae (Farjon 2005; Eckenwalder 2009). It is the only extant genus thought to be represented by anatomically preserved ovulate cones from the Cretaceous (Alvin 1960; Miller 1976a), and many ovulate cones from the Cretaceous

assigned to the organ-genus *Pityostrobus* strongly resemble pines (Miller 1976a). *Pinus* and Pinaceae are of outstanding ecological and economic importance and relatively detailed morphological descriptions are available for all extant species (e.g. Farjon 2005; Eckenwalder 2009). Furthermore, molecular systematic studies have clarified relationships among extant genera and species (Wang et al. 2000; Gernandt et al. 2008). However, our knowledge of the anatomical variation in living species of *Pinus* is incomplete. Miller (1976a) proposed generic concepts for living and fossil pinaceous cones based in part on the earlier work on living conifer species by Radais (1894) and in part on his reference collection, which at the time included 65 species from nine of the 11 Pinaceae genera (sensu Farjon 2005; Eckenwalder 2009). Anatomical descriptions for ovulate cones of most living species either do not exist or are unpublished. In contrast, anatomical descriptions are available for most fossil cones assigned to *Obirastrobus*, *Pityostrobus*, and *Pseudoaraucaria* (Miller 1976a; Smith and Stockey 2001, 2002).

Molecular phylogenetic studies strongly indicate that *Pinus* includes two monotypic subsections, both in *Pinus* subgenus *Strobus* (the soft pines): *Pinus* subsection *Krempfianae* is represented by *P. krempfii* Lecomte, endemic to central Vietnam, and *Pinus* subsection *Nelsoniae* is represented by *P. nelsonii* Shaw, a rare pinyon pine endemic to high desert woodlands of the Sierra Madre Oriental of Mexico (Fig. 1A; Gernandt et al. 2001; Syring et al. 2005; Parks et al. 2009). Neither species was available to Miller (1976a) when he proposed diagnostic features that fossil cones must possess to be classified in *Pinus* rather than *Pityostrobus*. As a result, the cone morphologies of two major lineages remained unknown. The present study's objectives are to describe the ovulate cone anatomy of *Pinus nelsonii* and to explore additions and modifications to an existing cone morphology matrix (Smith and Stockey 2001, 2002) that could clarify relationships among extant and fossil taxa. We split the generic-level terminal "*Pinus*" into three species-level terminals, divided several multistate characters into multiple characters, and added several external morphological characters for ovuliferous scales, bracts, and seeds.
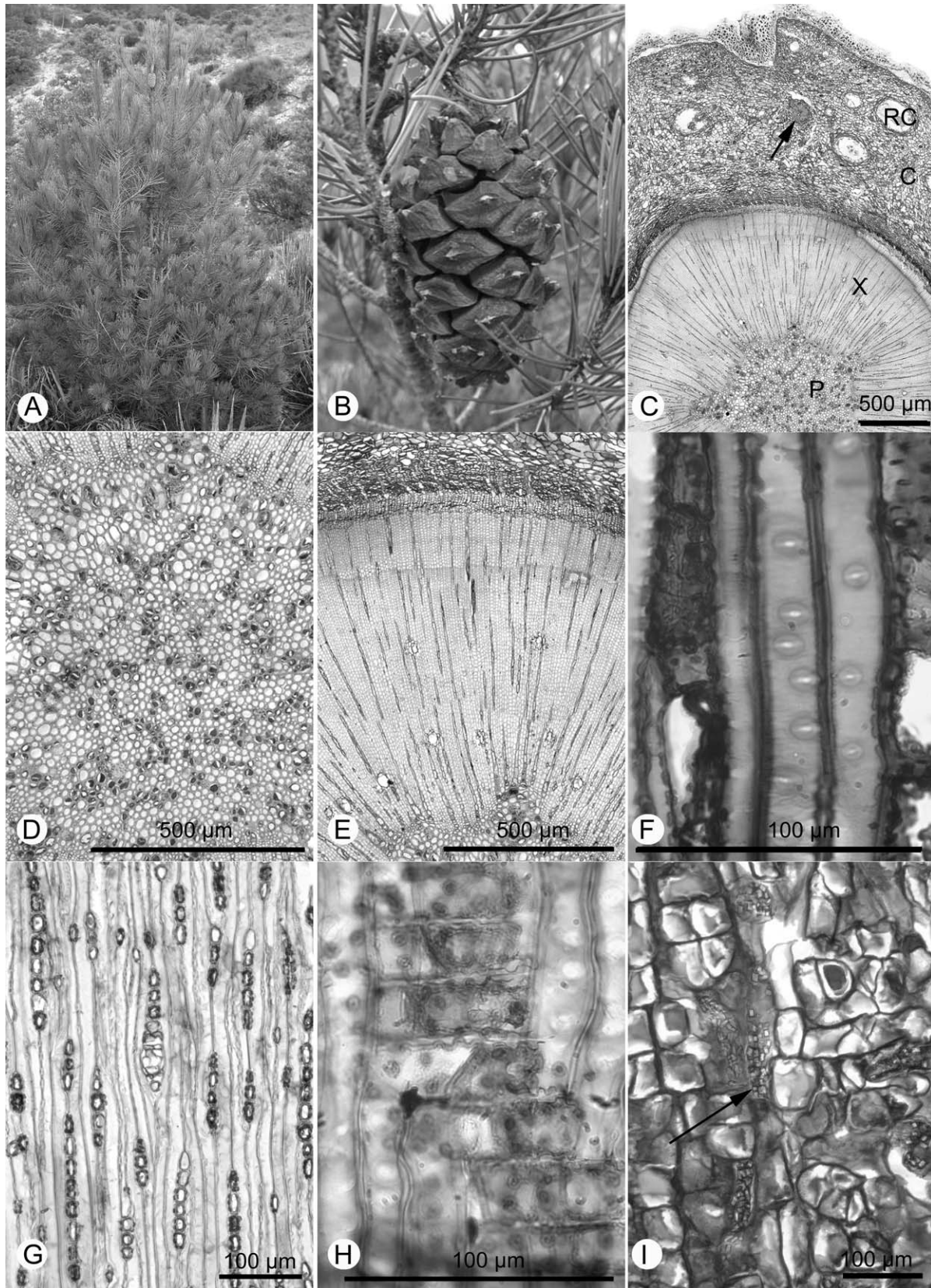
Fig. 1. *Pinus nelsonii*. A. Habit. An ovulate cone is visible at shoot apex. B. Mature ovulate cone. C-I. Composite images of sections of the peduncle. C-E. Transverse section (slide 499–001–006). C. View of pith, xylem, cortex, and periderm. A vascular bundle (arrow) is visible in the cortex. D. Enlarged view of pith with idioblasts. E. Enlarged view of secondary xylem and cambium showing rays and two indistinct rings of small resin ducts, as well as phloem and inner cortex. F-I. Longitudinal sections of the peduncle. F. Tangential section of the xylem showing axial tracheids with uniseriate circular bordered pits (slide 499–011–046). G. Tangential section showing uniseriate and biseriate xylem rays, and pits visible on the ray walls (slide 499–011–035). H. Radial section showing ray parenchyma with pitted walls and piceoid pits in the cross-fields (slide 499–011–051). I. Tangential section of cortex showing dark organic contents and prismatic crystals (arrow; slide 499–011–001). C = cortex, P = pith, RC = resin canal, X = xylem.

Materials and Methods

Branch, leaf, and cone collections of *Pinus nelsonii* were made from mature trees from a natural population in the municipio of Guadalcázar, San Luis Potosí on August 17, 2004 and December 13, 2009 (DSG Nos. 499 and 1095, vouchers deposited at MEXU). Two ovulate cones, one mature and the other immature, were rehydrated by soaking for 48–72 hrs in water. Scales from the basal, medial, and apical parts of the axis were removed from the mature cone, and a double-edged razor was used to make transverse and longitudinal sections of the immature cone. The material was soaked for one wk in 10% aqueous ethylene diamine at room temperature (Carlquist 1982), dehydrated in serial rinses of 70–100% ethanol, embedded in paraffin, and sectioned on a rotary microtome at 10–14 μm. Sections were stained with safranin and alcian blue (Ruzin 1999), cleared with CitriSolv (Fisher Scientific, Suwanee, Georgia), and mounted with Entellan rapid mounting medium (Merck, Whitehouse Station, New Jersey) for observation under a compound microscope at 5–100 × magnification. Means and standard deviations were calculated based on 25 measurements of tracheids and rays from serial sections of the mature cone. Images were captured with a Leica Firecam and stitched in Photoshop CS3 with the photomerge option. Original unmerged images are available from the first author upon request.

The cone morphology matrix of Smith and Stockey (2002) was reconstructed in Mesquite (Maddison and Maddison 2009), modified, and deposited in TreeBASE (study number 10553). The matrix included 50 taxa (Appendix 1). The outgroups used by Smith and Stockey (2001, 2002) were retained: two extant conifers, *Cryptomeria japonica* and *Sciadopitys verticillata*, and the fossil taxon *Pararaucaria patagonica*, the latter usually hypothesized as belonging to a conifer family outside Pinaceae (Stockey 1977). The taxon "*Pinus*", for which seven of thirty-tree characters were scored as polymorphic by Smith and Stockey (2002), was replaced with the extant species *Pinus nelsonii* and *Pinus ponderosa* (*Pinus* subgenus *Pinus*, a hard pine), and the fossil species *Pinus belgica*. Character states for *P. nelsonii* were from this study, those for *P. ponderosa* were based on observations from the reference collection of C. N. Miller, currently housed at the University of Alberta, and those for *P. belgica* were from Alvin (1960).

The character matrix was expanded and modified from Smith and Stockey (2002; Appendix 2). Some multistate characters from Smith and Stockey (2002) included the state "absent" together with alternative character forms (e.g. resin canal position in the scale). We separated these into two characters, one specifying the structure's presence or absence, and the other specifying its alternative forms (Hawkins et al. 1997; Sereno 2007). Those taxa scored as absent for the first character state were scored as inapplicable for the second. The parsimony searches did not treat inapplicable states differently than missing states; we distinguished between inapplicable and missing characters to make the matrix scoring clearer. Also, Smith and Stockey (2002) coded the distribution of resin canals and sclerenchyma in the scale with the states "abaxial," "adaxial," "between," and "both abaxial and adaxial." The alternative states can be found in the same taxa and implies that they are not homologous (conjunction coding; Patterson 1982). We separated these multistate characters into separate presence or absence characters (characters 26–36). This effectively divided one of Miller's (1976a) features used to delimit *Pinus* and *Pityostrobus* (resin canals at the scale base restricted to the abaxial side of the vascular tissue) into two characters.

Nine characters were added to the matrix: bract apex shape (character 18; Alvin 1988), vascular trace transverse shape in the ovuliferous scale distal to the seed (character 24; Alvin 1988), ovuliferous scale shape in surface view (character 37; Frankis 1989; see also Alvin 1988; Mente and Brack-Hanes 1992; Farjon 2005), shape of the ovulate scale base (character 38; Frankis 1989; Farjon 2005), ovuliferous scale umbo presence or absence (character 40; treated as separate from ovuliferous scales thickening distally; Smith and Stockey 2001, 2002), ovuliferous scale umbo position (character 41), seed body shape in surface view (character 51; Frankis 1989), presence or absence of a vascular trace entering the seed (character 52; Alvin 1988), and nature of seed wing attachment (character 54; Frankis 1989; see also Alvin 1988). Five multistate characters represented counts or measures and were treated as ordered (Appendix 2). Newly included characters for fossil cones and the outgroups were scored from published descriptions (Radais 1894; Dutt 1916; Alvin 1953, 1957a, 1957b, 1960; Creber 1956, 1960, 1967; Miller 1972, 1974, 1976a, 1976b, 1977, 1978, 1985; Miller and Robison 1975; Robison and Miller 1977; Stockey 1977, 1981; Crabtree and Miller 1989; Takaso and Tomlinson 1989, 1991; Ohsawa et al. 1991, Ohsawa and Nishida 1992; Falder et al. 1998; Ratzel et al. 2001; Smith and Stockey 2001, 2002).

The matrix included 54 parsimony-informative characters (Appendix 2) for a total of 2,700 cells, of which 219 cells (8.1%) were scored as miss-ing, 46 (1.7%) as polymorphic, and 65 (2.4%) as inapplicable. The extant ingroup taxa with the most missing, polymorphic, and inapplicable characters were *Picea* (nine polymorphic and one inapplicable), *Cathaya argyrophylla* (eight missing and one inapplicable), *Larix* (eight polymorphic and one inapplicable), and *Abies* (seven polymorphic and two inapplicable). Fossil ingroup taxa with the most missing and inapplicable characters were *Pseudoaraucaria benstedi* (18 missing), *Pityostrobus shastaensis* (12 missing), *Pityostrobus cliffwoodensis* (nine missing), and *Pityostrobus macrocephalus* (11 missing and one inapplicable). For the outgroups, *Pararaucaria patagonica* had five characters scored as missing, thirteen scored as inapplicable, and one as polymorphic, and *Cryptomeria japonica* had four characters scored as missing and eleven scored as inapplicable.

The matrix was analyzed in PAUP* (Swofford 2002) with equally weighted parsimony. Characters scored as polymorphic for a taxon were treated as polymorphic rather than uncertain (pset /mstaxa = polymorph). A heuristic search was performed with 100,000 random addition sequence replicates, tree-bisection reconnection (TBR) branch swapping, and saving 25 trees per replicate. The remaining search parameters were left on default. Branch support was estimated with 1,000 bootstrap replicates of a heuristic search with 50 random sequence addition replicates, TBR branch swapping, and saving 10 trees per random sequence addition replicate. Ancestral character states were reconstructed with parsimony in Mesquite.

Results

General Features—The external morphology of the ovulate cones conformed to previous descriptions given for the species (Farjon and Styles 1997). Mature cones were cylindrical, measured 5.3×3.6–10.8×5.0 cm and were supported on elongated recurved peduncles 0.5–1.0 cm in diameter and up to 4.1 cm in length (Fig. 1B). Ovuliferous scales were helically arranged, ca. 70–80 per cone and oriented approximately at a right angle to the cone axis. Scales separated slightly from one another to expose the seeds; they did not spread widely as is typical for the genus.

Cone Peduncle—Transverse sections of the peduncle were 8.5–9.3 mm in diameter. The pith was 2.0 ± 0.2 mm in diameter and composed of isodiametric thick walled parenchyma cells; scattered idioblasts with dark organic contents were also present. Intercellular spaces were visible (Figs. 1C and 1D).

The vascular cylinder was 1.6 ± 0.1 mm thick (70–100 cells wide) from pith to cambium. The mature cone had three faint growth increments marked by a decrease in late wood tracheid radial dimensions but without an increase in wall thickness (Fig. 1E). Forty-four axial resin canals were present in transverse section, most occurring as two irregular rings in the early wood of the first growth increment, usually small (0.06 mm), and surrounded by approximately 7–10 thin-walled epithelial cells. No axial parenchyma was observed. Tracheids were 19.6 ± 2.1 μm in diameter and 840 ± 160 μm in height. The tracheid walls showed a transition from primary xylem with helical thickenings to metaxylem and secondary xylem with circular bordered pits with tori. The circular bordered pits were predominantly uniseriate (Fig. 1F), but occasionally biseriate and opposite.

Most xylem rays were uniseriate, but biseriate rays (with a radial resin canal) were also present (Fig. 1G). Uniseriate rays were 7.25 ± 6.71 (1–30) cells and 169 ± 155 μm tall and 16.3 ± 3.7 μm wide. Biseriate rays were 12.1 ± 2.8 cells and 263 ± 76 μm tall and 43 ± 9.0 μm wide. Rays were homocellular with pitted transverse walls. The cross-fields of tracheids with ray cells typically had two to four (much less frequently one or five) piceoid pits per cross-field (Fig. 1H).

The cambial-phloem zone was 0.25–0.6 mm (15 cells) thick with exclusively nonlignified cells. The cortex was 1.5 ± 0.4 mm thick, composed of irregularly shaped parenchyma cells with

walls of varying thickness. Distributed throughout the cortex were 52 axial resin canals varying in diameter from 0.06×0.06 mm to 0.8×0.4 mm and surrounded by 12–17 thin-walled epithelial cells (Fig. 1C). Two circular vascular bundles occurred in the cortex. Some cells in the cortex contained dark organic contents, and some of these had prismatic crystals (Fig. 1I). The phelloderm consisted of two to three rows of rectangular, sclerified cells, and exterior to them, a phellem of eight to 11 cell layers (Fig. 1C).

Cone Axis—The cone axis was 9.6 cm long, 8.5–10.0 mm in diameter at its base, slightly wider medially, and tapering apically. Near the cone base, the pith was 2.1 ± 0.1 mm in diameter and composed principally of isodiametric thick-walled parenchyma cells, occasionally with dark organic contents, crystals, or both (Fig. 2A). Scattered sclerenchyma and idioblasts were also present; resin canals were absent. The pith increased to 2.9 ± 0.1 mm at the medial part of the cone.

The vascular cylinder (Fig. 2B) was 1.3 ± 0.1 mm thick at the base and successively thinner apically (1.1 mm at the medial part of the cone). The vascular cylinder was continuous except where vasculature led to bract-scale complexes (Fig. 2C). Three faint growth increments were present in the xylem (visible at the axis base), delimited by two indistinct rings of resin canals. Each canal was surrounded by approximately 7–10 thin-walled epithelial cells (Fig. 2B). Tracheids were 15.7 ± 3.6 µm in diameter, with uniseriate and occasionally biseriate and opposite circular bordered pits (Fig. 2D). Uniseriate rays were 3.32 ± 4.16 (one to 17) cells and 90.8 ± 114 µm tall and 15.8 ± 4.8 µm wide. Rays were homocellular. Ray cells had walls with large pits (Fig. 2E). Near the primary xylem both procumbent and upright ray cells were present, giving way to procumbent cells in the later-formed secondary xylem. Two to four (rarely one or five) pits occurred in the cross-fields (Fig. 2F). These pits were interpreted as pinoid because the pit apertures lacked wide borders (IAWA Committee 2004).

The cortex was of uneven width, interrupted by vascular traces; midway between the cone base and apex its maximum width was 2.07 ± 0.12 mm (54 ± 5.3 cells; Fig. 2A). It was composed of parenchyma cells and resin canals. No sclerenchyma was observed. The resin canals decreased in number apically (there were 26 canals midway from the base to the apex), varied in diameter from 0.08–0.24 mm, and were surrounded by one to several layers of thin-walled epithelial cells. There were 12–17 cells in the innermost layer.

Cone Scale Complex—Vascular traces leading to the bract-scale complex were cylindrical, fused at their origin in the inner cortex of the axis, and contained small resin canals (Fig. 2G). In the outer cortex, the traces separated into a scale and bract trace that were abaxially concave and circular in transverse section, respectively; these were accompanied abaxially by two resin canals (Fig. 2H). The bract and scale remained fused a short distance beyond the cone axis and the single scale trace diverged into three separate traces; a row of resin canals was abaxial to the scale traces and two resin canals were lateral to the bract trace (Fig. 2I). The scale and subtending bract separated first at their lateral margins.

The bracts were minute, 1.5–2.5 mm long, and 2.4–3.7 mm wide × 0.5 mm tall at their base (Fig. 2I). The bract apex was thin with a broad, round to slightly pointed margin. Bract cells were parenchymatous. A vascular trace entered the center of the bract and extended for more than half the bract length. Two small resin canals extended into the free part of the bract on both sides of the trace.

The ovuliferous scales were elongate, cuneate to obovate in surface view, and terminated in a prominent apophysis with a transversely keeled dorsal umbo and a minute mucro that was worn almost flat. The basal and apical scales were small and sterile, while those from the medial part of the cone measured ca. 1.8–2.5 cm long and 1.3–2.2 cm wide at their widest point near the apex. Scales bore two seeds in depressions on their adaxial surface separated by an overarching interseminal ridge. One seed was aborted in some scales.

Most cells in the scales were parenchyma. Near the scale base the vascular traces divided, forming a row near the adaxial surface (Fig. 3A). At seed level, the vascular traces were visibly curved on the phloem side (abaxially concave) in transverse section (Fig. 3B) and remained near the adaxial surface (Fig. 3C). Distal to the seeds, vascular traces were arranged in a row midway between the abaxial and adaxial surface and were more prominently curved (Fig. 3D). Resin canals were abaxial to (and inside) the traces at the scale base. At seed level they also occurred between, and adaxial to the vascular bundles; several also occurred in a prominent medial ridge that overarched the two seed cavities (Fig. 3C). Distally, resin canals were distributed throughout the scale tissue, with larger canals near the lateral margins (Fig. 3D).

Seeds were obovoid, 10.5–14.8 mm long and 6.8–9.1 mm wide and surrounded by a thick (1.0–1.3 mm) seed coat. Effective seed wings were absent, but vestigial wing tissue surrounded the distal end and lateral sides of the seed in the position corresponding to wing attachment in other *Pinus* species. This tissue usually remained attached to the scale upon removing the seed, forming a 2–3 mm ridge around the seed cavity. Embryos were 8–9 mm long with 11–14 cotyledons.

Phylogenetic Analysis—The heuristic search recovered a single most parsimonious tree with a length (L) of 306 steps, a consistency index for informative characters (CI) of 0.37 and a retention index (RI) of 0.60. The shortest tree length was found in 11 of the 100,000 random addition sequence replicates. Only seven branches received bootstrap support greater than 50% (Fig. 4). Outgroup rooting with *Sciadopitys* and *Cryptomeria* recovered *Pararaucaria* (of uncertain familial affinity) within Pinaceae. The root was located between *Larix* + *Pseudotsuga* and the rest of Pinaceae. Pinaceae also included an "Abietoid" clade comprised of the extant genera *Abies*, *Cedrus*, *Keteleeria*, *Pseudolarix*, and *Tsuga* together with *Pararaucaria*, *Pseudoaraucaria*, and nine *Pityostrobus* species. A second "Pinoid" clade comprised the extant genera *Cathaya*, *Picea*, and *Pinus* together with 18 *Pityostrobus* species. All six species of the fossil genus *Pseudoaraucaria* were recovered as monophyletic and sister to *Abies*. Both species of *Obirastrobus* also formed a clade. The three *Pinus* species were paraphyletic to ten *Pityostrobus* species (*P. andraei*, *P. argonnensis*, *P. bernissartensis*, *P. hautrageanus*, *P. jacksonii*, *P. kayeii*, *P. lynnii* *P. macrocephalus*, *P. palmeri*, and *P. shastaensis*).

There were six characters with no homoplasy (consistency index = 1) on the most parsimonious tree (Fig. 4). Seed wings formed from sarcotestal tissue (character 47) united the outgroups *Sciadopitys* and *Cryptomeria*. The multistate character for bract length (character 16) united *Sciadopitys* and *Cryptomeria* (equal to scale length), and *Larix* and *Pseudotsuga* (longer than scale length). Bract length was optimized as shorter than scale length in the Abietoid and Pinoid clades, but the character was scored as polymorphic in several genera (both longer and shorter in *Abies*, *Larix*, *Pseudolarix*, and *Tsuga*). Had these taxa been divided into multiple species
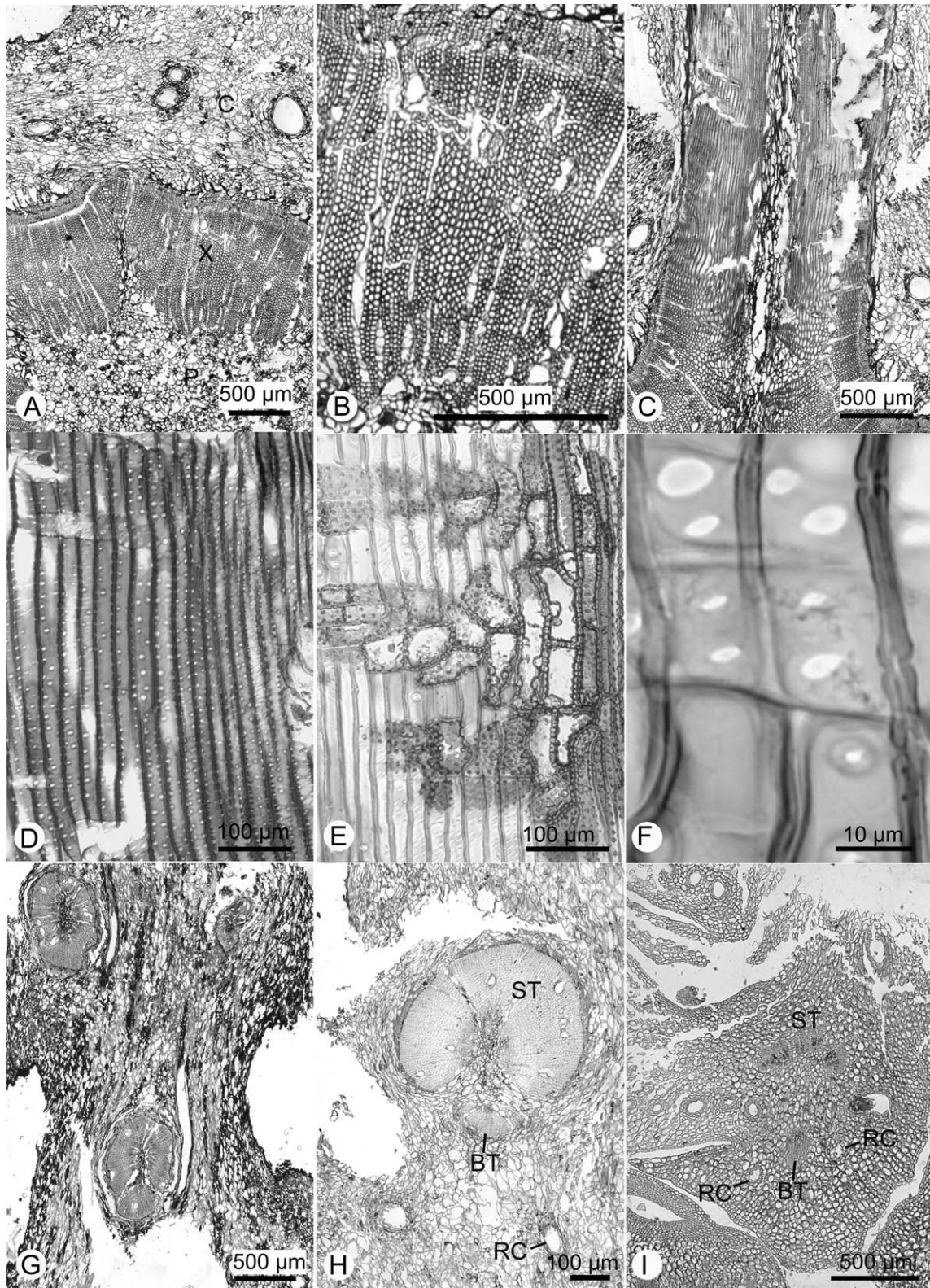
FIG. 2.   Composite images of sections of the cone axis of *Pinus nelsonii*. A-C. Transverse sections of the cone axis midway between the base and apex (slide 499–003–001). A. View of pith, xylem, phloem, and cortex. B. Enlarged view of xylem with resin canals surrounded by thin walled epithelial cells (many are torn). Faint growth increments are visible as differences in tracheid diameters. C. View of vascular trace originating in the pith and passing through secondary xylem and into the cortex. D-H. Longitudinal sections through the axis. D. Radial section through xylem in medial part of cone showing tracheids with uniseriate circular bordered pits (slide 499–013–002). E. Radial section through xylem at base of cone showing ray cells undergoing a change of orientation (slide 499–023–001). F. Radial section through xylem at medial part of cone showing ray parenchyma cells and cross-fields with pinoid pits (slide 499–022–006). G. Tangential section through the inner cortex showing fusion of the scale and bract trace (slide 499–013–003). H. Tangential section through the middle-outer cortex showing abaxially concave scale trace, bract trace, and two abaxial resin canals (slide 499–012–085). I. Transverse section through the bract-scale complex of an immature cone showing a bract with a single vascular trace and two resin canals (slide 1095–006–051). BT = bract trace, C = cortex, P = pith, RC = resin canal, ST = scale trace, X = xylem.
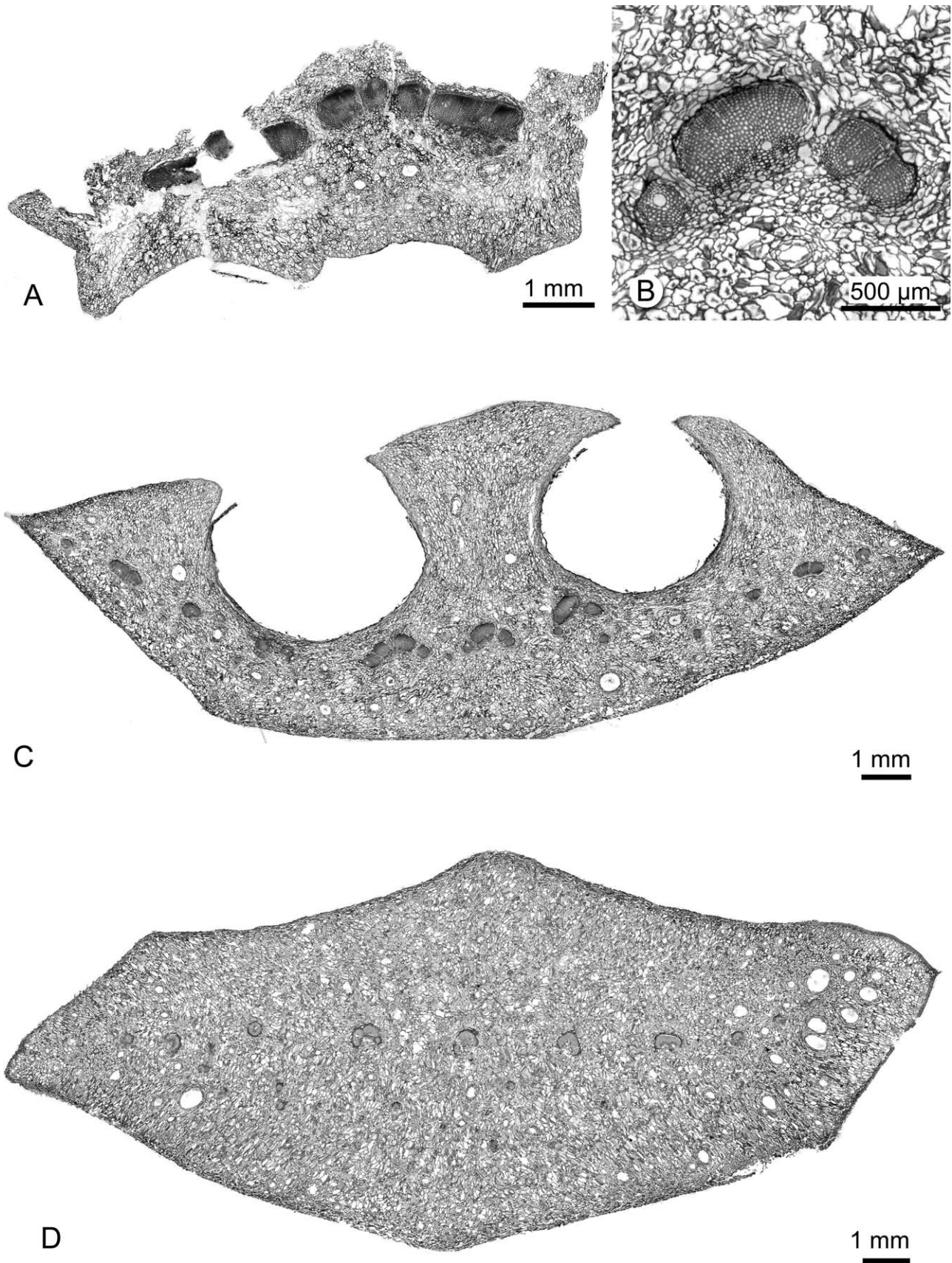
FIG. 3.   Composite images of transverse sections of a medial cone scale of *Pinus nelsonii*. A. Scale base showing resin canals abaxial to and within the vascular bundles. At the lateral margins of the scale, canals occur close to the adaxial surface (slide 499–006–010). B. Enlarged view of a vascular bundle showing curvature (slide 499–007–018). C. Transverse section of a medial scale at the level of the seed showing the prominent interseminal ridge and resin canals abaxial to, between, adaxial to, and within the vascular bundles (slide 499–007–018). D. Distal to seed the vascular traces are abaxially concave and form a row across the middle of the scale (slide 499–008–001).
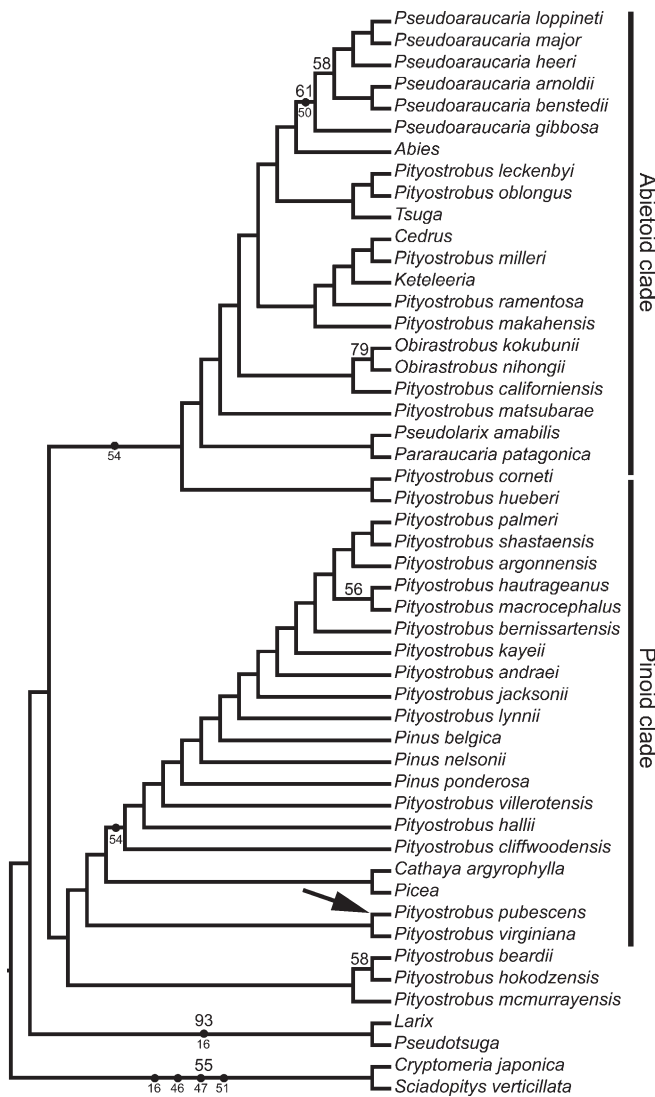
FIG. 4. Relationships in Pinaceae inferred from a cladistic analysis of cone morphology characters. The single most parsimonious tree (L = 306 steps, CI = 0.37, RI = 0.60). Bootstrap values > 50% are above branches. Closed circles denote characters with no homoplasy on the tree mapped to their corresponding branches using parsimony ancestral state reconstruction in Mesquite. Character numbers below the circles are as follows: 16 = bract length, 46 = seed wings from sarcotestal tissue, 47 = seed wings from scale tissue, 50 = enlarged parenchyma pad at chalazal end of seed, 51 = number of ovules per scale, and 54 = mode of seed wing attachment. The arrow indicates the position of the root when deleting the six fossil taxa with the most missing or inapplicable data. More details of the ancestral state construction and the analyses that gave alternative rootings are provided in the text.

terminals the character would have exhibited homoplasy. There were two synapomorphies for Pinaceae + *Pararaucaria* (character 46; seed wings formed from ovuliferous scale tissue and character 51; two seeds per ovuliferous scale, scored as polymorphic in *Pararaucaria*), a synapomorphy for the six *Pseudoaraucaria* species (character 50; an enlarged parenchyma pad or cushion present at the chalazal end of the seed), and a multistate character supporting the monophyly of part of the Abietoid clade including *Abies* and *Keleeria*, and of *Pinus* + 14 *Pityostrobus* species (character 54; seed wing attachment forming deep cups or claws, respectively). There were multiple equally most parsimonious reconstructions for this character; its location in Fig. 4 placed transformations as close as

possible to the root. The most homoplasious characters on the trees were primarily anatomical rather than external morphological characters. Those with a consistency index less than 0.2 were presence or absence of bract sclerenchyma (character 19; CI = 0.14), abaxially concave versus straight vascular bundles distally in the ovuliferous scales (character 24; CI = 0.14), presence or absence of resin canals in the ovuliferous scales between the vascular tissue at the level of the seed body (character 29; CI = 0.12), presence or absence of resin canals in the ovuliferous scales adaxial to vascular tissue at the level of the seed body (character 30; CI = 0.14), presence or absence of sclerenchyma in the ovuliferous scales between the vascular tissue (character 35; CI = 0.091), and presence or absence of sclerenchyma in the ovuliferous scales adaxial to the vascular tissue (character 36; CI = 0.11).

Mapping character transformations onto the tree (favoring reversions with accelerated transformation) showed which characters united *Pinus* with thirteen *Pityostrobus* species (the node including *Pityostrobus cliffwoodensis*). There were three character transformations at that branch: bract and ovuliferous scale separating first medially (character 15; CI = 0.22, homoplastic in the same clade), resin canals to ovuliferous scales between vascular tissue abaxial at level of seed (character 29; CI = 0.14, homoplastic in the same clade), and seed wings attached by claws (character 54; CI = 1.0, scored as missing in several *Pityostrobus* species and with equally parsimonious reconstructions on other branches). The characters used by Miller (1976a) to separate *Pinus* from *Pityostrobus* had low consistency indices. The separation or fusion of bract traces at their origin (character 10; CI = 0.50) required four steps on the tree and would have required three more steps to account for polymorphic taxa (Fig. 5A). The fused state (as in *Pinus*) was inferred as derived seven times and lost once. The transverse shape of the scale vascular scale bundles distal to the seeds (character 24; CI = 0.14) required seven steps on the tree, with the abaxially concave state (as in *Pinus*) inferred as derived four times and lost three times (Fig. 5B). The presence or absence of resin canals at the scale base abaxial to the vascular traces (character 26; CI = 0.25) required four steps on the tree, with presence inferred as derived twice and lost twice (Fig. 5C). The presence or absence of resin canals at the scale base adaxial to the vascular traces (character 27; CI = 0.20) required five steps on the tree, with presence inferred as ancestral, being lost four times and regained once (Fig. 5D). The scale apex thinning or thickening distally (character 39; CI = 0.20) required five steps on the tree, with the thickening state inferred as derived four times and lost once (Fig. 5E).

We evaluated whether including taxa with many characters scored as missing or inapplicable affected the placement of species for which more information was available. *Pararaucaria patagonica* and *Cryptomeria japonica* lacked resin canals, which resulted in 10 characters scored as inapplicable. Deleting these two taxa resulted in a matrix with three variable but parsimony-uninformative characters and 50 parsimony-informative characters. The heuristic search recovered 24 trees (L = 292, CI excluding uninformative characters = 0.37, RI = 0.60). The strict consensus (not shown) was less resolved, with the Abietoid and Pinoid clades collapsing into a polytomy, although the groups supported by bootstrap greater than 50% in Fig. 4 were recovered. The position of the root changed, with *Pityostrobus pubescens* sister to the rest of Pinaceae. We further deleted four ingroup taxa that were described from fossils with abraded scale apices (*Pityostrobus*
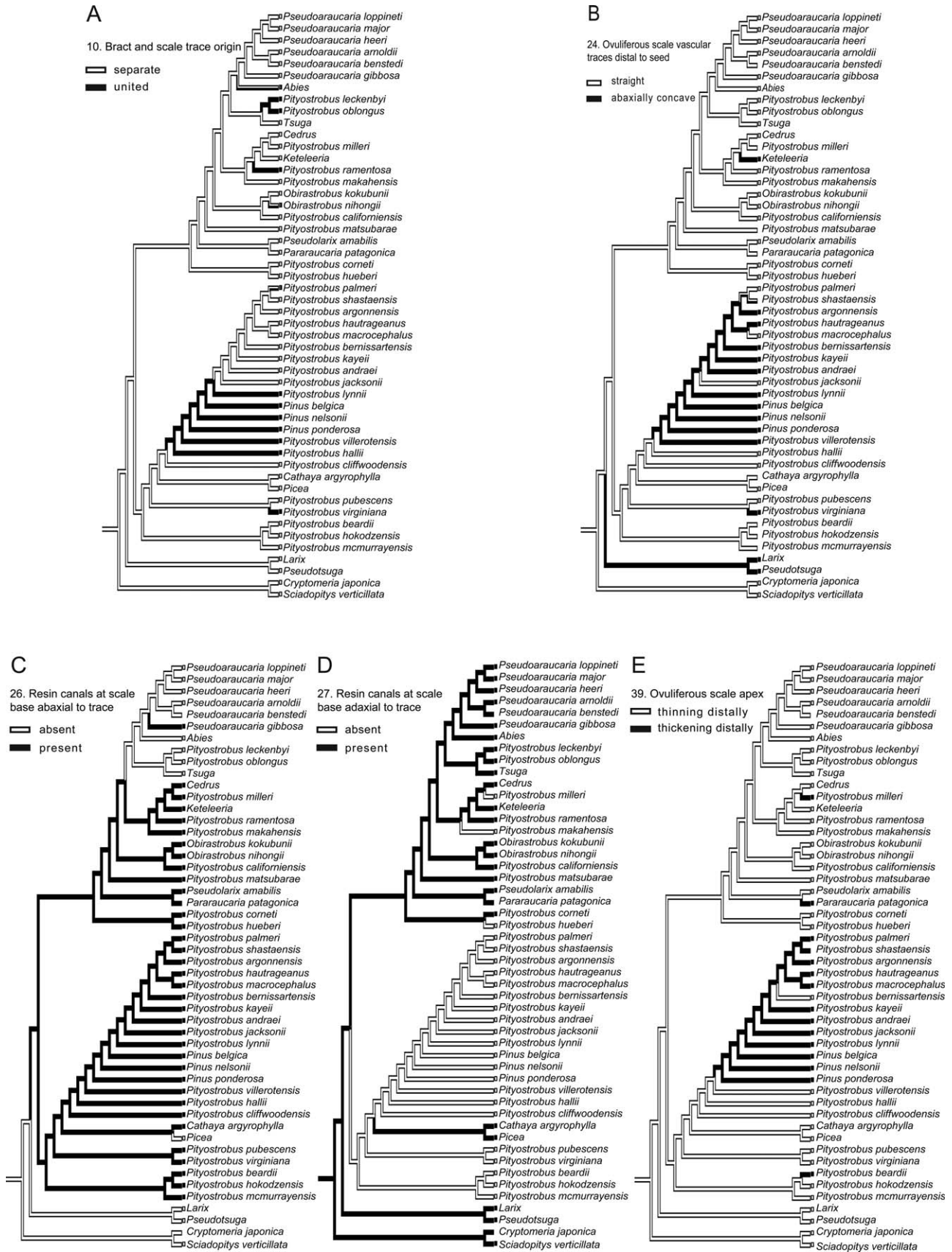
Fig. 5. Parsimony character state reconstructions for ovulate cone characteristics used to delimit *Pinus* from *Pityostrobus*. A. Bract and scale trace origin (character 10) separate (white) or united (black). B. Ovuliferous scale vascular trace transverse shape distal to seed (character 24) straight (white) or abaxially concave (black). C. Resin canals abaxial to ovuliferous scales at scale base (character 26) absent (white) or present (black). D. Resin canals adaxial to ovuliferous scales at scale base (character 27) absent (white) or present (black). E. Ovuliferous scale apex (character 39) thinning distally (white) or thickening distally (black). Taxa with polymorphic states are half black and half white.

cliffwoodensis, *Pityostrobus macrocephalus*, *Pityostrobus shastaensis*, and *Pseudoaraucaria benstedii*). The resulting matrix had three variable but parsimony-uninformative characters and 49 parsimony-informative characters. A heuristic search recovered 32 trees (L = 287, CI excluding uninformative characters = 0.38, RI = 0.59). In the strict consensus (not shown), *Larix* and *Pseudotsuga* were recovered in the same clade as *Picea*, *Cathaya*, *Pinus*, and 17 *Pityostrobus* species, and *Pinus* was paraphyletic to only two *Pityostrobus* species (*P. hallii* and *P. villerotensis*), although another nine *Pityostrobus* species occurred with them in a more inclusive clade. Relationships were less resolved among *Cedrus*, *Abies*, *Keteleeria*, *Pseudolarix*, *Tsuga*, *Pseudoaraucaria*, and other *Pityostrobus* species. The Pinaceae root again was located between *Pityostrobus pubescens* and the rest of the family.

Discussion

Diagnostic Characters, Phylogeny, and Natural Groups— Miller (1976a, p. 114) used "four features that are highly characteristic of *Pinus*" ovulate cone to delimit the genus; these were confirmed as present in *P. nelsonii*: 1) inflated scale apices (character 39; Fig. 5E), 2) resin canals at the scale base restricted to the abaxial side of the vascular traces (coded as two characters, 26 and 27; Figs. 5C and 5D), 3) abaxially concave traces in the distal part of the scale (character 24; Fig. 5B), and 4) vascular traces to the bract and scale united at their origin (character 10; Fig. 5A). Miller (1976a) proposed that fossil permineralized cones must possess all four features to be included in the genus. The presence of these characters in *Pinus nelsonii* is consistent with Miller's delimitation of the genus and does not provide additional evidence that the concept of *Pinus* ovulate cones ought to be expanded to include particular fossils assigned to *Pityostrobus*.

The consensus tree reported in this study (Fig. 4) is more resolved and more robust (as measured by bootstrap values) than the strict consensus reported by Smith and Stockey (2002). Several of the same groups were recovered; for example the sister relationships among pairs of *Pityostrobus* species and the *Pseudoaraucaria* clade. There was also some agreement between our strict consensus tree and their majority-rule tree. In particular, Smith and Stockey (2002) recovered *Pinus* (as a single terminal) monophyletic with five *Pityostrobus* species (*P. lynnii*, *P. cliffwoodensis*, *P. jacksonii*, *P. kayeii* and *P. virginiana*). Except for *Pityostrobus virginiana*, the same *Pityostrobus* species (and others) grouped with *Pinus* here. The relationships we recovered for extant taxa were also more resolved, but they disagreed in several respects from those recovered in molecular studies (e.g. Wang et al. 2000; Gernandt et al. 2008). For example, *Pseudotsuga* and *Larix* are sister to *Picea*, *Cathaya*, and *Pinus* in most molecular studies. The results here suggest which *Pityostrobus* species will most profitably be included in future analyses of *Pinus*, and that further progress will be made once more generic-level terminals like *Abies* and *Picea* are divided into multiple species-level terminals.

The phylogenetic analysis (Fig. 4) supports Miller's (1976a) assertion that many but not all *Pityostrobus* species may be more closely related to *Pinus* than to any other living genus. Some fossil cones assigned to *Pityostrobus* have a superficial resemblance to *Pinus* but have been excluded from the genus because they lack one or more of the four ovulate cone features (Miller 1976a; Smith and Stockey 2001, 2002). Miller (1976a) recognized that three of the four features are homopla-

sious, occurring in phylogenetically disparate extant Pinaceae species. Among extant genera, only inflated scale apices are unique to *Pinus* (Fig. 5E). In contrast, the cone axis base in the living species *Abies lasiocarpa* (Hook.) Nutt. and *Tsuga canadensis* Carrière has bract and scale traces that are fused at their origin as in *Pinus* (Miller 1976a). Curved traces in the distal part of the scale were reported from four extant genera, *Pinus*, *Larix*, *Pseudotsuga*, and *Keteleeria* (Alvin 1988; Fig. 5B). Although *Pinus* and three other genera (*Cathaya*, *Cedrus*, and *Keteleeria*) have resin canals abaxial to the trace at the bract-scale origin (Fig. 5C), *Pinus* is the only extant genus with the combination of abaxial resin canals present and adaxial resin canals absent (Figs. 5C and 5D). Widespread homoplasy in pinaceaous ovulate cone characters suggests that few monophyletic groups in Pinaceae will be characterized by unreversed synapomorphies.

Previous workers have suggested that at least one of the four ovulate cone features diagnostic for *Pinus* is actually absent in some species of the genus. In particular, *Pinus bungeana* Zucc. ex Endl. (subsection *Gerardianae*), and *P. albicaulis* Engelm. and *P. lambertiana* Douglas (subsection *Strobus*) were interpreted as having their vascular traces to the bract and scale separate at their origin (Miller 1992; Saiki 1996). If confirmed, these *Pinus* species would share the same three of four characters as *Pityostrobus andraei*, *P. argonnensis*, and *P. kayeii*. *Pityostrobus argonnensis* and a few other species currently assigned to *Pityostrobus* were originally described as *Pinus*. Many fossil species have been included in *Pityostrobus* rather than *Pinus* because they lack one of these characters, effectively treating the characters as homoplasious in *Pityostrobus* but not in *Pinus*. This practice arguably has promoted an artificial classification, and assignments to *Pityostrobus* have sometimes been made with workers expressing the need for a more natural classification (Alvin 1957b).

Potentially Informative Morphological Characters within Pinus—Variable macromorphological and anatomical characters in ovulate cones of extant and fossil pines are potential synapomorphies for infrageneric groups. A terminal scale umbo is a synapomorphy for *Pinus* subsection *Strobus* (Saiki 1996; Gernandt et al. 2005). And although homoplasy explains the shared presence of a prominent interseminal ridge overarching the seeds in *Pinus nelsonii* and the distantly related fossil genus *Pseudoaraucaria*, similar enlargement occurs in species of *Pinus* subsection *Cembroides*. Many pines rely on animals rather than wind to disperse their seeds, and an enlarged interseminal ridge may prevent the large, functionally wingless seeds from being passively released once the scales separate. The pinyon pine character syndrome, which includes a low habit, and cones with large, functional wingless, bird dispersed seeds, may be responsible for morphological similarities between *Pinus nelsonii* and its close relatives in *Pinus* subsection *Cembroides*. Such pinyon pine characters may have a similar distribution throughout the genus (Gernandt et al. 2005). Although subject to convergence, the characters are informative at lower levels as "local synapomorphies."

Cortex sclerenchyma has been reported for species in the extant hard pine subsections *Pinus*, *Contortae*, and *Australes*, but it also occurs in the oldest fossil pines (Miller 1976a; Saiki 1996). Other variable characters identified in previous works (Smith and Stockey 2001, 2002) include presence or absence of pith sclerenchyma, the number of growth increments in the secondary xylem of the axis, presence or absence of marked cortex resin canal dilation at branching points to the bracts

and scales, presence or absence of bract sclerenchyma, presence or absence of a bract vascular trace, and presence or absence of resin canals between and adaxial to the vascular traces in the scales at the level of the seeds. In general, these anatomical characters were found to be homoplasious, but further taxonomic sampling may reveal that they are informative at less inclusive levels.

Resin canals occur within the scale vascular traces in *P. nelsonii* and some other *Pinus* species. Two other species in subgenus *Strobus*, *Pinus monophylla* Torr. and Frém. and *P. bungeana*, also have resin canals in the vascular traces, as do some members of subgenus *Pinus* (e.g. *P. radiata* D. Don), suggesting that this is another homoplasious character. Two distinct rings of resin canals also occur in the traces of *Pinus princetonensis* Stockey from the Eocene of British Columbia (Stockey 1984), which is similar to section *Pinus*.

Regarding wood characters, growth increments observed in *P. nelsonii*, although faint, are characteristic of *Pinus* and the distantly related genus, *Cedrus*, both of which develop their cones over two or more years. Axial resin canals present in the wood of *P. nelsonii* are common in Pinaceae, having been reported from one or more species of all genera except *Keteleeria*, *Pseudolarix*, and *Tsuga* (Miller 1976a). Ray features have been emphasized for their diagnostic value in conifers (Greguss 1955, 1972) and described for *Pinus nelsonii* (Huerta Crespo 1963), but their taxonomic distribution in ovulate cones needs further study.

The present study fills an important gap in our knowledge of cone anatomical variation among *Pinus* subsections and identifies which fossil cones currently classified in the polyphyletic genus *Pityostrobus* may be closely related to *Pinus*. The expanded cone morphology data matrix continues to support the monophyly of *Obirastrobus* and *Pseudoaraucaria*, but their phylogenetic placement in Pinaceae remains unclear. A more robust phylogenetic hypothesis for fossil ovulate cones and extant genera may reveal new insights into the timing and sequence of evolution in Pinaceae. Further progress in understanding relationships between extant and fossil species is possible by including more taxa and characters in phylogenetic analyses. Dividing generic terminals into species terminals to avoid scoring characters as polymorphic is under way, as is adding characters not only from cones, but from other structural and molecular sources.

LITERATURE CITED

Alvin, K. L. 1953. Three abietaceous cones from the Wealden of Belgium. *Institut Royal des Sciences Naturelles de Belgique Memoires* 125: 1–42.

Alvin, K. L. 1957a. On *Pseudoaraucaria* Fliche emend., a genus of fossil pinaceous cones. *Annals of Botany* 21: 33–51.

Alvin, K. L. 1957b. On the two cones *Pseudoaraucaria heeri* (Coemans) nov. comb. and *Pityostrobus villerotensis* nov. sp. from the Wealden Formation of Belgium. *Institut Royal des Sciences Naturelles de Belgique Memoires* 135: 1–27.

Alvin, K. L. 1960. Further conifers of the Pinaceae from the Wealden Formation of Belgium. *Institut Royal des Sciences Naturelles de Belgique Memoires* 146: 1–39.

Alvin, K. L. 1988. On a new specimen of *Pseudoaraucaria major* Fliche (Pinaceae) from the Cretaceous of the Isle of Wight. *Botanical Journal of the Linnean Society* 97: 159–170.

Carlquist, S. 1982. The use of ethylenediamine in softening hard plant structures for paraffin sectioning. *Stain Technology* 57: 311–317.

Crabtree, D. R. and C. N. Miller. 1989. *Pityostrobus makahensis*, a new species of silicified pinaceous seed cone from the middle Tertiary of Washington. *American Journal of Botany* 76: 176–184.

Creber, G. T. 1956. A new species of abietaceous cone from the Lower Greensand of the Isle of Wight. *Annals of Botany* 20: 375–383.

Creber, G. T. 1960. On *Pityostrobus leckenbyi* (Carruthers) Seward and *Pityostrobus oblongus* (Lindley & Hutton) Seward, fossil abietaceous cones from the Cretaceous. *Botanical Journal of the Linnean Society* 56: 421–429.

Creber, G. T. 1967. Notes on some petrified cones of the Pinaceae from the Cretaceous. *Proceedings of the Linnean Society of London* 178: 147–152.

Dutt, C. P. 1916. *Pityostrobus macrocephalus*, L. and H.: a Tertiary cone showing ovular structures. *Annals of Botany* 30: 529–549.

Eckenwalder, J. E. 2009. *Conifers of the world: the complete reference*. Ed. 1. Portland: Timber Press.

Falder, A. B., G. W. Rothwell, G. Mapes, R. H. Mapes, and L. A. Doguzhaeva. 1998. *Pityostrobus milleri* sp. nov., a pinaceous cone from the Lower Cretaceous (Aptian) of southwestern Russia. *Review of Palaeobotany and Palynology* 103: 253–261.

Farjon, A. 2005. *Pines: drawings and description of the genus Pinus*. Ed. 2. Leiden: Brill.

Farjon, A. and B. T. Styles. 1997. *Pinus (Pinaceae). Flora Neotropica Monograph 75*. New York: New York Botanical Garden.

Frankis, M. P. 1989. Generic inter-relationships in Pinaceae. *Notes from the Royal Botanic Gardens Edinburgh* 45: 527–548.

Gernandt, D. S., G. Gaeda López, S. Ortiz García, and A. Liston. 2005. Phylogeny and classification of *Pinus*. *Taxon* 54: 29–42.

Gernandt, D. S., A. Liston, and D. Piñero. 2001. Variation in the nrDNA ITS of *Pinus* subsection *Cembroides*: implications for molecular systematic studies of pine species complexes. *Molecular Phylogenetics and Evolution* 21: 449–467.

Gernandt, D. S., S. Magallón, G. Geada López, O. Zerón Flores, A. Willyard, and A. Liston. 2008. Use of simultaneous analyses to guide fossil-based calibrations of Pinaceae phylogeny. *International Journal of Plant Sciences* 169: 1086–1099.

Greguss, P. 1955. *Identification of living gymnosperms on the basis of xylotomy*. Budapest: Akadémiai Kiadó.

Greguss, P. 1972. *Xylotomy of the living conifers*. Budapest: Akadémiai Kiadó.

Hawkins, J. A. 2000. A survey of primary homology assessment: different botanists perceive and define characters in different ways. Pp. 22–53 in *Homology & systematics: coding characters for phylogenetic analysis*, eds., R. W. Scotland and R. T. Pennington. London and New York: Taylor & Francis.

Hawkins, J. A., C. E. Hughes, and R. W. Scotland. 1997. Primary homology assessment, characters and character states. *Cladistics* 13: 275–283.

Hennig, W. 1966. *Phylogenetic systematics*. Urbana: University of Illinois Press.

Huerta Crespo, J. 1963. Anatomia de la madera de 12 especies de coniferas mexicanas. *Instituto Nacional de Investigaciones Forestales. Boletin Técnico* 51: 1–51.

IAWA Committee. 2004. IAWA list of microscopic features for softwood identification. *IAWA Journal* 25: 1–70.

Maddison, W. P. and D. R. Maddison. 2009. Mesquite: a modular system for evolutionary analysis. Version 2.74 http://mesquiteproject.org.

Mente, R. F. and S. D. Brack-Hanes. 1992. A new pinaceous seed-cone from the Miocene of Idaho. *Botanical Journal of the Linnean Society* 108: 333–344.

Miller, C. N. Jr. 1972. *Pityostrobus palmeri*, a new species of petrified conifer cones from the Late Cretaceous of New Jersey. *American Journal of Botany* 59: 352–358.

Miller, C. N. Jr. 1974. *Pityostrobus hallii*, a new species of structurally preserved conifer cones from the Late Cretaceous of Maryland. *American Journal of Botany* 61: 798–804.

Miller, C. N. Jr. 1976a. Early evolution in the Pinaceae. *Review of Palaeobotany and Palynology* 21: 101–117.

Miller, C. N. Jr. 1976b. Two new pinaceous cones from the Early Cretaceous of California. *Journal of Paleontology* 50: 821–832.

Miller, C. N. Jr. 1977. *Pityostrobus lynni* (Berry) comb. nov., a pinaceous seed cone from the Paleocene of Virginia. *Bulletin of the Torrey Botanical Club* 104: 5–9.

Miller, C. N. Jr. 1978. *Pityostrobus cliffwoodensis* (Berry) comb. nov., a pinaceous seed cone from the Late Cretaceous of New Jersey. *Botanical Gazette (Chicago, Ill.)* 139: 284–287.

Miller, C. N. Jr. 1985. *Pityostrobus pubescens*, a new species of pinaceous cones from the Late Cretaceous of New Jersey. *American Journal of Botany* 72: 520–529.

Miller, C. N. Jr. 1992. Structurally preserved cones of *Pinus* from the Neogene of Idaho and Oregon. *International Journal of Plant Sciences* 153: 147–154.

Miller, C. N. Jr. and C. R. Robison. 1975. Two new species of structurally preserved pinaceous cones from the Late Cretaceous of Martha's Vineyard Island, Massachusetts. *Journal of Paleontology* 49: 138–150.

Nixon, K. C. and J. J. Davis. 1991. Polymorphic taxa, missing values and cladistic analysis. *Cladistics* 7: 211–233.

Ohsawa, T., H. Nishida, and M. Nishida. 1991. Structure and affinities of the petrified plants from the Cretaceous of northern Japan and Saghalien VII: a petrified pinaceous cone from the Upper Cretaceous of Hokkaido. *Journal of Japanese Botany* 66: 356–368.

Ohsawa, M. N. and H. Nishida. 1992. Structure and affinities of the petrified plants from the Cretaceous of northern Japan and Saghalien. XII. *Obirastrobus* gen. nov., petrified pinaceous cones from the Upper Cretaceous of Hokkaido. *Journal of Plant Research* 105: 461–484.

Parks, M., R. Cronn, and A. Liston. 2009. Increasing phylogenetic resolution at low taxonomic levels using massively parallel sequencing of chloroplast genomes. *BMC Biology* 7: 84.

Patterson, C. 1982. Morphological characters and homology. Pp. 21–74 in *Problems of phylogenetic reconstruction*, eds. K. A. Joysey and A. E. Friday. London and New York: Academic Press.

Pleijel, F. 1995. On character coding for phylogenetic reconstruction. *Cladistics* 11: 309–315.

Radais, M. 1894. Contribution a l'étude de l'anatomie comparée du fruit des conifères. *Annales des Sciences Naturelles Botanique Sér* 7: 165–368.

Ratzel, S. R., G. W. Rothwell, G. Mapes, R. H. Mapes, and L. A. Dohuzhaeva. 2001. *Pityostrobus hokodzensis*, a new species of pinaceous cone from the Cretaceous of Russia. *Journal of Paleontology* 75: 895–900.

Ruzin, S. E. 1999. Plant microtechnique and microscopy. New York: Oxford University Press.

Robison, C. R. and C. N. Miller Jr. 1977. Anatomically preserved seed cones of the Pinaceae from the Early Cretaceous of Virginia. *American Journal of Botany* 64: 770–779.

Saiki, K. 1996. *Pinus mutoi* (Pinaceae), a new species of permineralized seed cone from the Upper Cretaceous of Hokkaido, Japan. *American Journal of Botany* 83: 1630–1636.

Sereno, P. C. 2007. Logical basis for morphological characters in phylogenetics. *Cladistics* 23: 565–587.

Shang, H., J. Z. Cui, and C. S. Li. 2001. *Pityostrobus yixianensis* sp. nov., a pinaceous cone from the Lower Cretaceous of north-east China. *Botanical Journal of the Linnean Society* 136: 427–437.

Smith, S. Y. and R. A. Stockey. 2001. A new species of *Pityostrobus* from the Lower Cretaceous of California and its bearing on the evolution of Pinaceae. *International Journal of Plant Sciences* 162: 669–681.

Smith, S. Y. and R. A. Stockey. 2002. Permineralized pine cones from the Cretaceous of Vancouver Island, British Columbia. *International Journal of Plant Sciences* 163: 185–196.

Stockey, R. A. 1977. Reproductive biology of the Cerro Cuadrado (Jurassic) fossil conifers: *Pararaucaria patagonica*. *American Journal of Botany* 64: 733–744.

Stockey, R. A. 1981. *Pityostrobus mcmurrayensis* sp. nov., a permineralized pinaceous cone from the Cretaceous of Alberta. *Canadian Journal of Botany* 59: 75–82.

Stockey, R. A. 1984. Middle Eocene *Pinus* remains from British Columbia. *Botanical Gazette (Chicago, Ill.)* 145: 262–274.

Swofford, D. L. 2002. PAUP*. Phylogenetic analysis using parsimony (*and other methods). ver. 4.0 beta 10. Sunderland: Sinauer Associates.

Syring, J., A. Willyard, R. Cronn, and A. Liston. 2005. Evolutionary relationships among *Pinus* (Pinaceae) subsections inferred from multiple low-copy nuclear loci. *American Journal of Botany* 92: 2086–2100.

Takaso, T. and P. B. Tomlinson. 1989. Aspects of cone and ovule ontogeny in *Cryptomeria* (Taxodiaceae). *American Journal of Botany* 76: 692–705.

Takaso, T. and P. B. Tomlinson. 1991. Cone and ovule development in *Sciadopitys* (Taxodiaceae-Coniferales). *American Journal of Botany* 78: 417–428.

Wang, X.-Q., D. C. Tank, and T. Sang. 2000. Phylogeny and divergence times in Pinaceae: evidence from three genomes. *Molecular Biology and Evolution* 17: 773–781.

Wiens, J. J. 2003. Missing data, incomplete taxa, and phylogenetic accuracy. *Systematic Biology* 52: 528–538.

APPENDIX 1. Taxa included in the cladistic analysis.

Extant generic level taxa: *Abies* Mill., *Cedrus* Trew, *Keteleeria* Carrière, *Larix* P. Mill., *Picea* A. Dietr., *Pseudotsuga* Carrière, *Tsuga* (Endlicher) Carrière (including *Nothotsuga* H. H. Hu ex C. Page, which is often recognized as a separate genus from *Tsuga*). Extant species level taxa: *Cathaya argyrophylla* Chun & Kuang, *Cryptomeria japonica* D. Don, *Pinus nelsonii* Shaw, *Pinus ponderosa* D. Douglas ex P. Lawson & C. Lawson, *Pseudolarix amabilis* Rehder, and *Sciadopitys verticillata* Siebold & Zucc. Fossil species: *Obirastrobus kokubunii* Ohsawa, Nishida & Nishida, *Obirastrobus nihongii* Ohsawa, H. Nishida & M. Nishida, *Pararaucaria patagonica* Wieland, *Pinus belgica* Alvin, *Pityostrobus andraei* (Coemans) Seward, *Pityostrobus argonnensis* (Fliche) Creber, *Pityostrobus beardii* Smith & Stockey, *Pityostrobus bernissartensis* (Alvin) Alvin, *Pityostrobus californiensis* Smith & Stockey, *Pityostrobus cliffwoodensis* (Berry) Miller, *Pityostrobus corneti* (Coemans) Alvin, *Pityostrobus hallii* Miller, *Pityostrobus hautrageanus* Alvin, *Pityostrobus hokodzensis* Ratzel et al., *Pityostrobus hueberi* Robison & Miller, *Pityostrobus jacksonii* Creber, *Pityostrobus kayeii* Miller & Robison, *Pityostrobus leckenbyi* (Carruthers) Seward, *Pityostrobus lynnii* (Berry) Miller, *Pityostrobus macrocephalus* Dutt, *Pityostrobus makahensis* Crabtree & Miller, *Pityostrobus mcmurrayensis* Stockey, *Pityostrobus matsubarae* Ohsawa, H. Nishida & M. Nishida, *Pityostrobus milleri* Falder et al., *Pityostrobus oblongus* (Lindley & Hutton) Seward, *Pityostrobus palmeri* Miller, *Pityostrobus pubescens* Miller, *Pityostrobus ramentosa* Miller, *Pityostrobus shastaensis* Miller, *Pityostrobus villerotensis* Alvin, *Pityostrobus virginiana* Robison & Miller, *Pseudoaraucaria arnoldii* Miller & Robison, *Pseudoaraucaria benstedi* (Mantell) Alvin, *Pseudoaraucaria gibbosa* (Coemans) Alvin, *Pseudoaraucaria heeri* (Coemans) Alvin, *Pseudoaraucaria loppineti* Fliche, *Pseudoaraucaria major* Fliche.

APPENDIX 2. Characters and their states. Characters and their states are from Smith and Stockey (2002), unless otherwise cited.

1. Pith sclerenchyma: 0 = absent; 1 = present. **2.** Pith resin canals: 0 = absent; 1 = present. **3.** Axis secondary xylem: 0 = forming a continuous cylinder (or little dissected); 1 = in separate strands. **4.** Axis secondary xylem axial resin canals: 0 = absent; 1 = present. **5.** Axis secondary xylem growth increments: 0 = one; 1 = two or more. **6.** Axis inner cortex sclerenchyma: 0 = absent; 1 = present. **7.** Axis outer cortex sclerenchyma: 0 = absent; 1 = present. **8.** Axis cortical resin canals diameter: 0 = uniform; 1 = dilated markedly near points of branching. **9.** Axis, scale, or bract base trichomes: 0 = absent; 1 = present. **10.** Bract and scale trace origin: 0 = separate; 1 = united. **11.** Ovuliferous scale trace derivation: 0 = from two lateral strands; 1 = from a single abaxially concave strand. **12.** Ovuliferous scale trace shape in inner cortex of axis: 0 = abaxially concave; 1 = becoming cylindrical after divergence. **13.** Resin canals to cone-scale complex arising from cortical canals: 0 = as a single branch; 1 = two origins; 2 = three separate origins; 3 = four separate origins; 4 = more than four separate origins. This character was treated as ordered. **14.** Bract and ovuliferous scale: 0 = fused; 1 = separating. The lack of separation of bract and scale is associated with a greatly reduced bract in *Pityostrobus andrei* and *Pityostrobus milleri*. In both species, the existence of the bract is inferred from the occurrence of a vascular trace in the topologically equivalent position (Alvin 1953; Falder et al. 1998). **15.** Bract and ovuliferous scale manner of separation: 0 = laterally first; 1 = medially first; 2 = all at once. This character was treated as unordered because no logical transformation series was apparent from the three states. **16.** Bract length relative to ovuliferous scale: 0 = shorter; 1 = equal in length; 2 = longer. This is ratio coding (Hawkins 2000). This character was treated as ordered. **17.** Bract base or cone-scale complex abaxial lobe: 0 = absent; 1 = present. **18.** Bract apex shape: 0 = simple; 1 = tridentate. **19.** Bract sclerenchyma: 0 = absent; 1 = present. **20.** Bract resin canals: 0 = absent; 1 = present. **21.** Bract resin canal number: 0 = two; 1 = more than two. **22.** Bract trace: 0 = entering bract; 1 = terminating before entering free part of bract. **23.** Bract trace vascular ray: 0 = absent; 1 = present. **24.** Ovuliferous scale vascular traces distal to seed: 0 = flat; 1 = abaxially concave. This character is from Miller (1976a). **25.** Ovuliferous scale resin canals: 0 = absent; 1 = present. **26.** Ovuliferous scale resin canals at scale base abaxial to vascular tissue: 0 = absent; 1 = present. This and the following resin canal distribution characters are modified from the coding of Smith and Stockey (2002). **27.** Ovuliferous scale resin canals at scale base adaxial to vascular tissue: 0 = absent; 1 = present. See note for preceding character. **28.** Ovuliferous scale resin canals at level of seed body abaxial to vascular tissue: 0 = absent; 1 = present. **29.** Ovuliferous scale resin canals at level of seed body between vascular tissue: 0 = absent; 1 = present. **30.** Ovuliferous scale resin canals at level of seed body adaxial to vascular tissue: 0 = absent; 1 = present. **31.** Ovuliferous scale resin canals distal to seed body (under wing and more distal sections) abaxial to

vascular tissue: 0 = absent; 1 = present. **32.** Ovuliferous scale resin canals distal to seed body between vascular tissue: 0 = absent; 1 = present. **33.** Ovuliferous scale resin canals distal to seed body adaxial to vascular tissue: 0 = absent; 1 = present. **34.** Ovuliferous scale sclerenchyma abaxial to vascular tissue: 0 = absent; 1 = present. **35.** Ovuliferous scale sclerenchyma between vascular tissue: 0 = absent; 1 = present. **36.** Ovuliferous scale sclerenchyma adaxial to vascular tissue: 0 = absent; 1 = present. **37.** Ovuliferous scale shape in surface view: 0 = flabellate (very broad at apex); 1 = round to rhomboid (broad in middle); 2 = tongue-shaped (elongate with linear sides, slightly broader at apex); 3 = subcordate; 4 = deltate triangular. This delimitation attempts to explicitly partition variation in shape (Alvin 1988; Mente and Brack-Hanes 1992; Gernandt et al. 2008). Mente and Brack-Hanes (1992) used broader than long, round, and elongate, corresponding to single structure ratio coding (Hawkins 2000). We used their definitions in preliminary analyses because it permitted scoring several fossils for which descriptions of overall scale shape was lacking. However, it forced us to group a diversity of shapes as elongate and we ultimately reverted to a coding similar to Gernandt et al. (2008). This character was treated as unordered because no logical transformation series was apparent among the states. **38.** Ovuliferous scale base: 0 = pedicillate; 1 = broad. This character was scored for extant taxa and for those fossils where the base of the ovuliferous scale was pictured, or dimensions provided (Frankis 1989). **39.** Ovuliferous scale apex: 0 = thinning distally; 1 = thickening distally. In contrast to Smith and Stockey (2001, 2002) we treated the presence or absence of an umbo as separate from a thickened scale apex; this allowed us to differentiate between the thin scale apices with umbos of *Pseudoaraucaria* from the thickened scale apices with umbos of *Pinus* and some *Pityostrobus*. **40.** Ovuliferous scale umbo: 0 = absent; 1 = present. See note for preceding character. **41.** Ovuliferous scale umbo position: 0 = dorsal; 1 = terminal. See Farjon (2005). **42.** Ovuliferous scale interseminal ridge between seeds: 0 = absent; 1 = present. Interseminal ridge absence was united with interseminal ridge length by Smith and Stockey (2002). Here it was separated into a presence/absence character and a length character (below). **43.** Ovuliferous scale interseminal ridge length relative to seed diameter: 0 = less than half of seed diameter; 1 = more than half of seed diameter; 2 = between and overarching seeds. This character is an example of ratio coding (Hawkins 2000). This character was treated as ordered. **44.** Ovuliferous scales at right angles to cone axis for length of seed body with sharply upturned distal portion: 0 = absent; 1 = present. **45.** Method of cone seed release: 0 = cone spreading; 1 = scale abscission from cone axis. **46.** Seed wings formed from ovuliferous scale tissue: 0 = absent; 1 = present. This character was modified with respect to Smith and Stockey (2002), who scored the sarcotestal wing in the outgroup taxa as an alternative state; in order to treat the two wing types as non-homologous, they have been scored as separate characters. **47.** Seed wings formed from sarcotestal tissue: 0 = absent; 1 = present. See preceding character. **48.** Resin vesicles or cavities in integument (seed coat): 0 = absent; 1 = present. **49.** Ridged sclerotesta: 0 = absent; 1 = present. **50.** Seed with enlarged parenchyma pad or cushion at chalazal end: 0 = absent; 1 = present. **51.** Ovules per ovuliferous scale: 0 = one; 1 = two: 2 = three or more. This character was treated as ordered. **52.** Seed body shape in surface view: 0 = ovoid to obovate; 1 = triangular to cuneate. This character is from Frankis (1989). **53.** Seed trace: 0 = absent; 1 = present. This character is from Alvin (1988). **54.** Seed wing attachment: 0 = deep cup; 1 = shallow cup; 2 = claws. This character is from Frankis (1989) and reflects the degree of attachment of seed wings to the scale. It was treated as ordered. States were scored as missing for most fossils because they were either unavailable or difficult to interpret.